Cell Host & Microbe, Volume *29*

Supplemental information

Uncoupling of IL-6 signaling and LC3-associated phagocytosis drives immunoparalysis during sepsis

Tonia Akoumianaki, Katerina Vaporidi, Eleni Diamantaki, Frédéric Pène, Remi Beau, Mark S. Gresnigt, Marina Gkountzinopulou, Maria Venichaki, Elias Drakos, Jamel El-Benna, George Samonis, Kieu T.T. Le, Vinod Kumar, Dimitrios Georgopoulos, Frank L. van de Veerdonk, Mihai G. Netea, Jean-Paul Latge, and Georgios Chamilos

Fig. S1

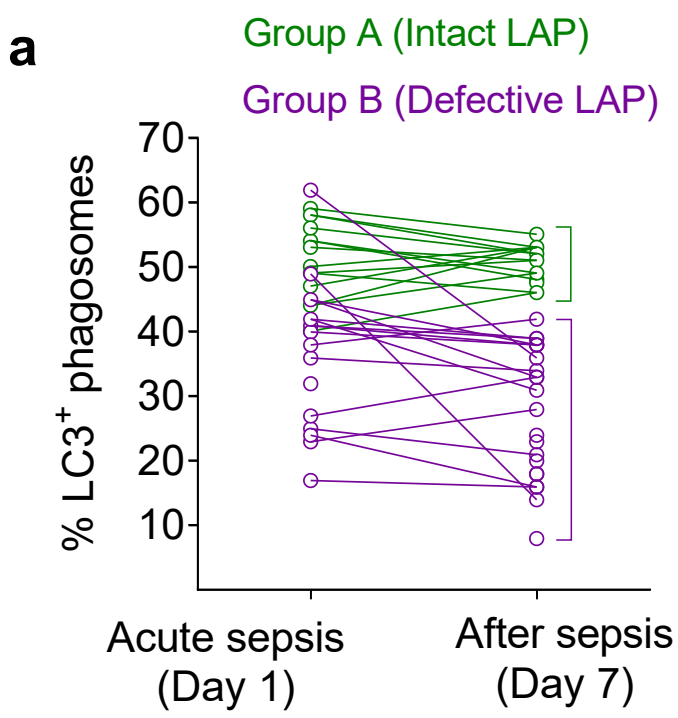
a
Group A (Intact LAP)
Group B (Defective LAP)
% LC3+ phagosomes
70
60
50
40
30
20
10
Acute sepsis
(Day 1)
After sepsis
(Day 7)

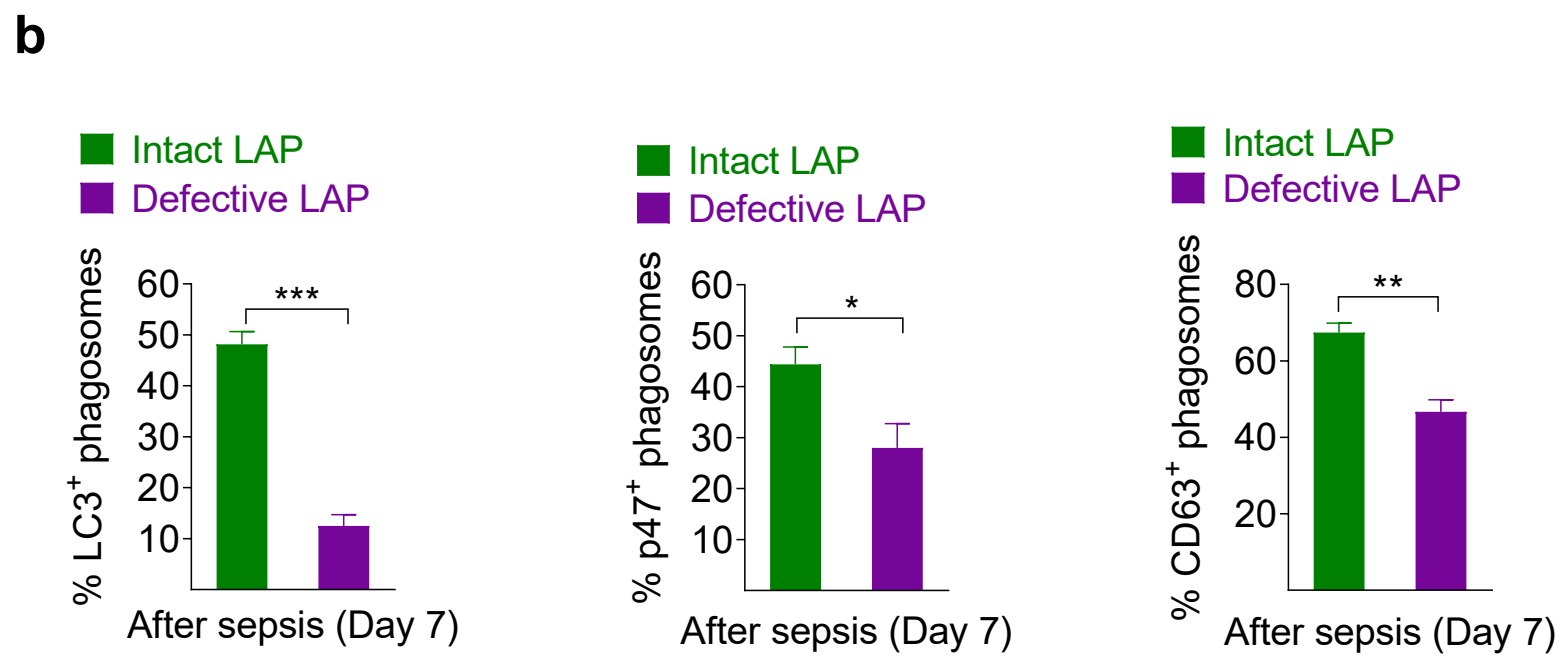
b
Intact LAP
Defective LAP
% LC3+ phagosomes
***
After sepsis (Day 7)
Intact LAP
Defective LAP
% p47+ phagosomes
*
After sepsis (Day 7)
Intact LAP
Defective LAP
% CD63+ phagosomes
**
After sepsis (Day 7)

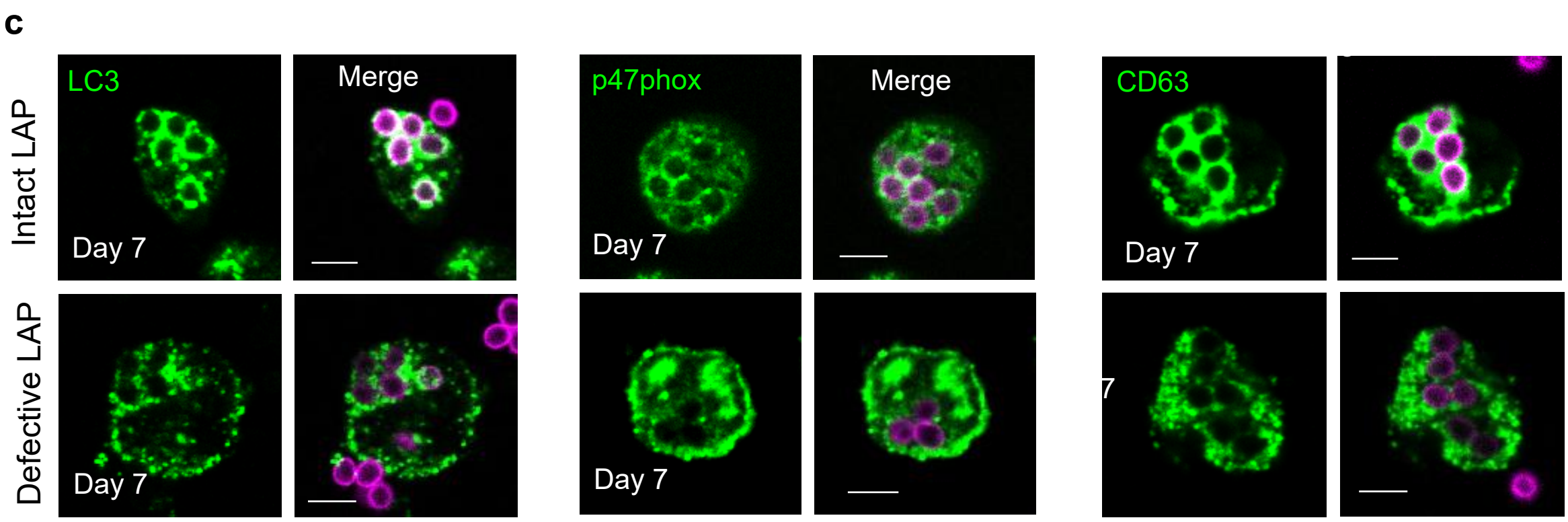
c
Intact LAP
Defective LAP
LC3
Merge
p47phox
Merge
CD63
Day 7

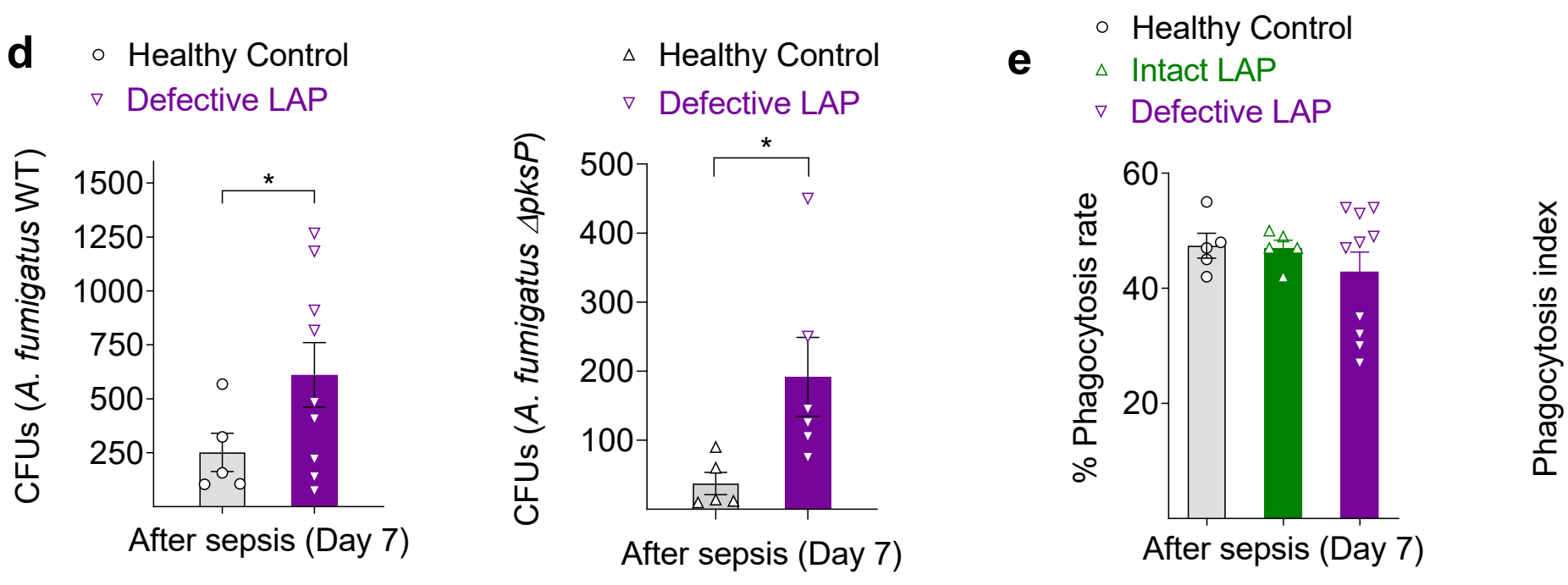
d
Healthy Control
Defective LAP
CFUs (A. fumigatus WT)
*
After sepsis (Day 7)
Healthy Control
Defective LAP
CFUs (A. fumigatus ΔpksP)
*
After sepsis (Day 7)
e
Healthy Control
Intact LAP
Defective LAP
% Phagocytosis rate
After sepsis (Day 7)
Healthy Control
Intact LAP
Defective LAP
Phagocytosis index
After sepsis (Day 7)

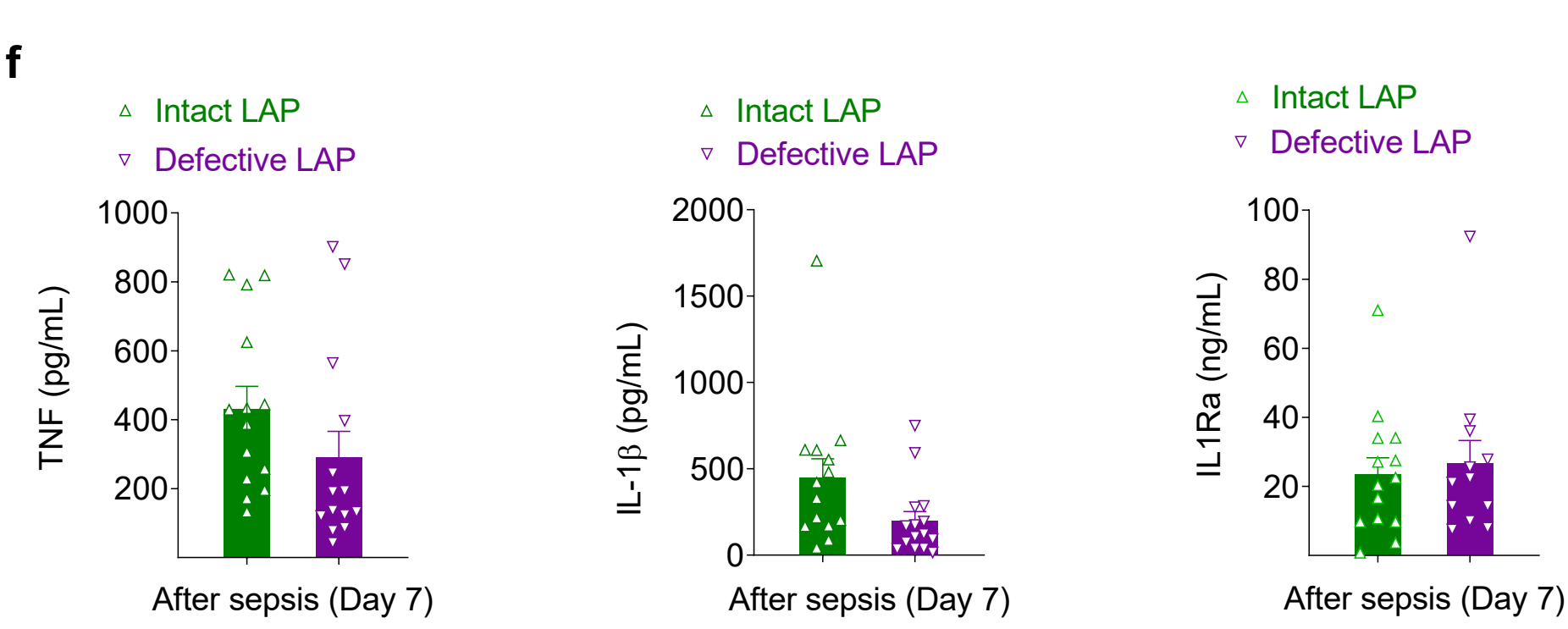
f
Intact LAP
Defective LAP
TNF (pg/mL)
After sepsis (Day 7)
Intact LAP
Defective LAP
IL-1β (pg/mL)
After sepsis (Day 7)
Intact LAP
Defective LAP
IL1Ra (ng/mL)
After sepsis (Day 7)

Fig. S1, related to Fig. 1. Studies on phagosome biogenesis and monocyte effector functions in sepsis patients with different LAP responses.

(**a)** Primary human $CD14^+$ monocytes obtained on the day of sepsis diagnosis (Day 1) and upon sepsis recovery (Day 7) were stimulated for 30 min with FITC-labeled conidia of *A. fumigatus* melanin-deficient Δ*pksP* strain (MOI 3:1), fixed, stained for LC3 and analyzed by confocal microscopy. Data on differences in LAPosome formation in monocytes of 38 consecutive patients over time (Day 1 vs. Day 7) are shown. Segregation of LAP responses in two distinct groups of patients (intact LAP vs. defective LAP) on Day 7 is shown with different colors.

(b) Data on quantification of $LC3^+$, $p47phox^+$, and $CD63^+$ phagosomes in monocytes obtained from a patient with defective LAP vs. a patient with intact LAP responses following recovery from sepsis (Day 7), stimulated as in (a) are presented as mean ± SEM. At least > 200 phagosomes were counted for each phagosome marker per patient. ***$p < 0.0001$, **$p < 0.001$, * $p < 0.01$, unpaired Student's t test.

(c) Representative immunofluorescent images of $LC3^+$ phagosome (LAPosome) formation, p47phox, and CD63 lysosomal protein recruitment to the phagosome of monocytes obtained from the patients analyzed in b are shown. FITC-labeled *A. fumigatus* conidia are shown in magenta; LC3, p47phox, and CD63 were stained with $Alexa^{555}$ secondary antibody and are shown in green. Scale bar, 5 μm.

(d) $CD14^+$ primary human monocytes obtained from healthy control (HC) individuals or sepsis patients with LAP defects were infected with conidia of wild type *Aspergillus fumigatus* (ATCC46645) or the melanin-deficient *A. fumigatus* strain Δ*pksP* at a MOI 1:10 upon sepsis recovery (Day 7). Killing of intracellular conidia was assessed following cell lysis at 24h by CFU counting. *$p < 0.01$, unpaired Student's t test.

(e) Phagocytosis rate and phagocytosis index of *Aspergillus* conidia by monocytes of HC or patients with sepsis stratified based on LAP responses upon stimulation at a MOI of 1:1 for 1h with conidia of Δ*pksP* melanin-deficient strain.

(f) Cytokine (TNF, IL-1β, IL-1Ra) production in culture supernatants following overnight stimulation of monocytes of patients with or without LAP defects with *Aspergillus* conidia, stimulated as in Fig. 1f. Each symbol represents mean value of each individual patient.

Fig. S2

a

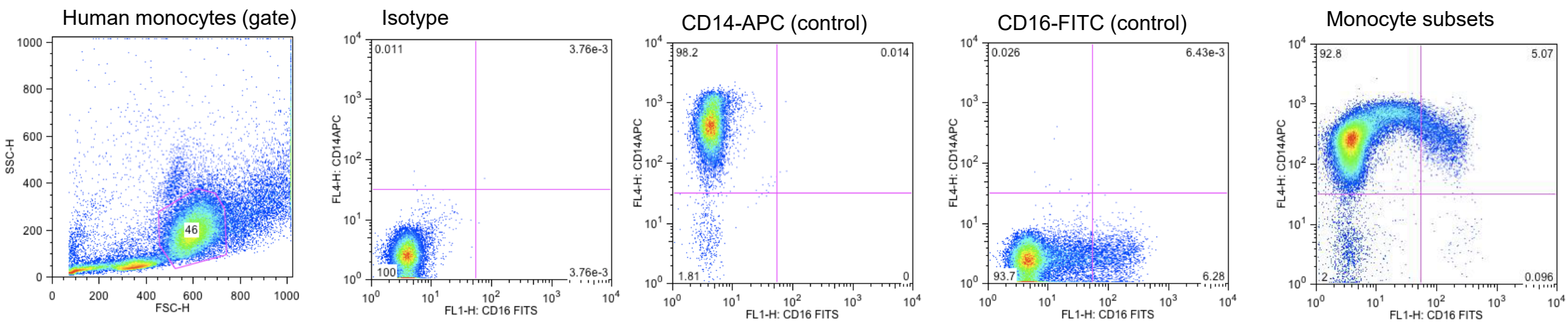
Human monocytes (gate)
SSC-H
FSC-H
46
Isotype
FL4-H: CD14APC
FL1-H: CD16 FITS
0.011
3.76e-3
100
3.76e-3
CD14-APC (control)
98.2
0.014
1.81
0
CD16-FITC (control)
0.026
6.43e-3
93.7
6.28
Monocyte subsets
92.8
5.07
2
0.096

b

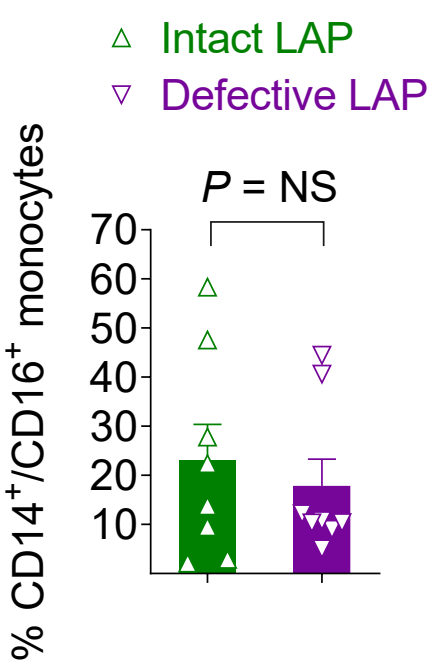
Intact LAP
Defective LAP
P = NS
% CD14+/CD16+ monocytes

c

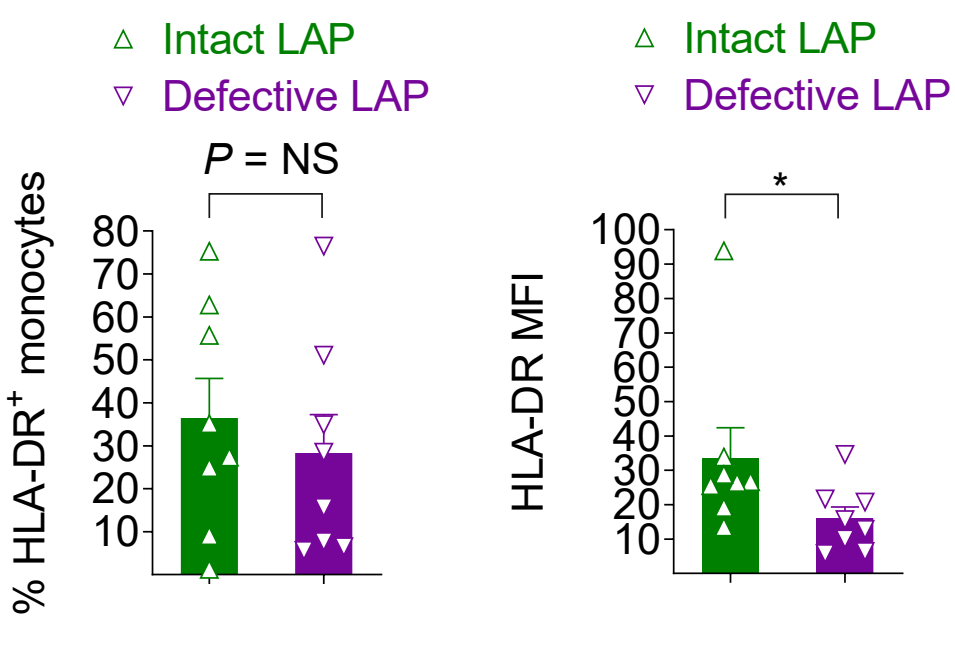
Intact LAP
Defective LAP
P = NS
% HLA-DR+ monocytes
Intact LAP
Defective LAP
*
HLA-DR MFI

d

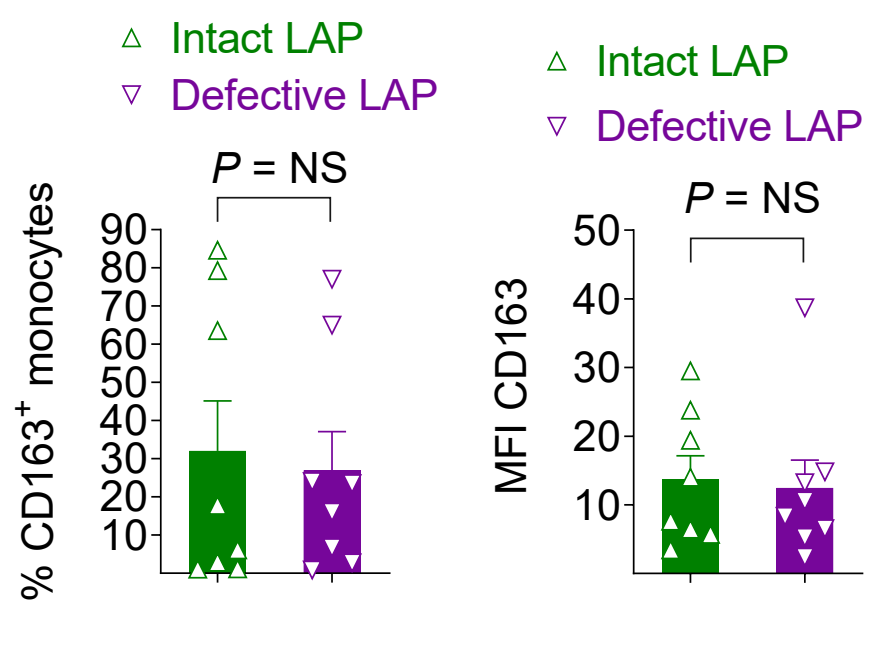
Intact LAP
Defective LAP
P = NS
% CD163+ monocytes
Intact LAP
Defective LAP
P = NS
MFI CD163

Fig. S2 related to Fig. 1. Flow cytometry analysis in monocytes of sepsis patients with different LAP responses.

(a) Gating strategy for analysis of human monocyte subsets in the peripheral blood of patients with sepsis.

(b) Differences in the percentage of $CD14^+CD16^+$ monocytes in a representative cohort of sepsis patients with intact or defective LAP responses. Each symbol represents mean value of the percentage of $CD14^+CD16^+$ monocytes of an individual patient.

(c) Differences in the percentage and mean fluorescence intensity (MFI) of HLA-DR and CD163 expression in $CD14^+$ monocytes obtained from sepsis patients with intact or defective LAP responses. * $p < 0.05$, unpaired Student's t test.

Fig. S3

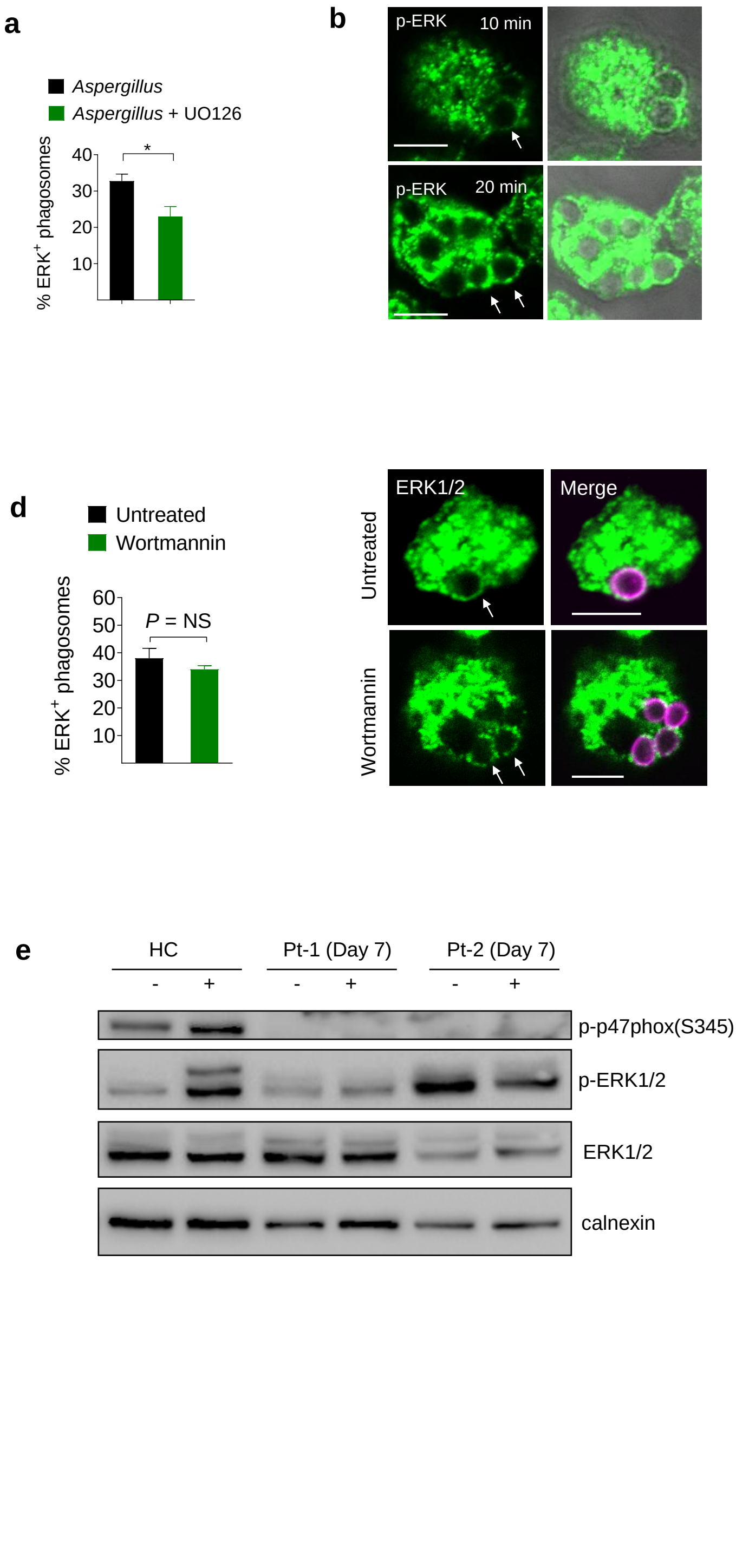
a
Aspergillus
Aspergillus + UO126
% ERK+ phagosomes
40
30
20
10
*
b
p-ERK
10 min
p-ERK
20 min
c
Untreated
Wortmannin
% LC3+ phagosomes
80
60
40
20
***
d
Untreated
Wortmannin
% ERK+ phagosomes
60
50
40
30
20
10
P = NS
ERK1/2
Merge
Untreated
Wortmannin
e
HC
Pt-1 (Day 7)
Pt-2 (Day 7)
-
+
-
+
-
+
p-p47phox(S345)
p-ERK1/2
ERK1/2
calnexin

Fig. S3 related to Fig. 2. Studies on mechanism of activation of ERK signaling in monocytes from healthy controls (HC) and sepsis patients.

(a) ERK^{+} phagosomes in monocytes infected with *Aspergillus* with or without pretreatment with the MEK1/2 inhibitor UO126 presented as mean ± SEM of one out of three independent experiments performed in triplicate. **p < 0.001, *p < 0.01, unpaired Student's t test.

(b) Representative immunofluorescence images of ERK1/2 phosphorylation on *Aspergillus*-containing phagosomes of human monocytes from HC stimulated as in (b). p-ERK was stained with the use of secondary $Alexa^{488}$ antibody (green). White arrows demonstrate p-ERK localization on the phagosome.

(c, d) Primary human monocytes from HC were stimulated as in (a) and either left untreated or treated with wortmannin (250 nM), a VPS34 (PI3K class III) inhibitor, added at 5 min of infection. LAPosome formation **(c)** and ERK recruitment **(d)** at *Aspergillus* phagosomes were evaluated at 30 min of infected and presented as mean ± SEM of one out of three independent experiments performed in triplicate. ***p < 0.0001, unpaired Student's t test. Representative immunofluorescence images of ERK recruitment to the phagosome (white arrows) are shown. ERK stained with $Alexa^{555}$ secondary antibody is shown in green and FITC-labeled *Aspergillus* conidia are shown in magenta. Scale bar, 5 μm**.**

(e) Primary human monocytes obtained from HC or patients following recovery from sepsis with evidence of LAP blockade and ERK phagosomal trafficking defects shown in **Fig. 2 (i-k),** were left untreated or stimulated for 20 minutes with *Aspergillus.* Phosphorylation of ERK1/2, p47phox *(*Ser345) and total ERK1/2 were determined in cell lysates by immunoblot analysis. Calnexin was used as loading control.

Fig. S4

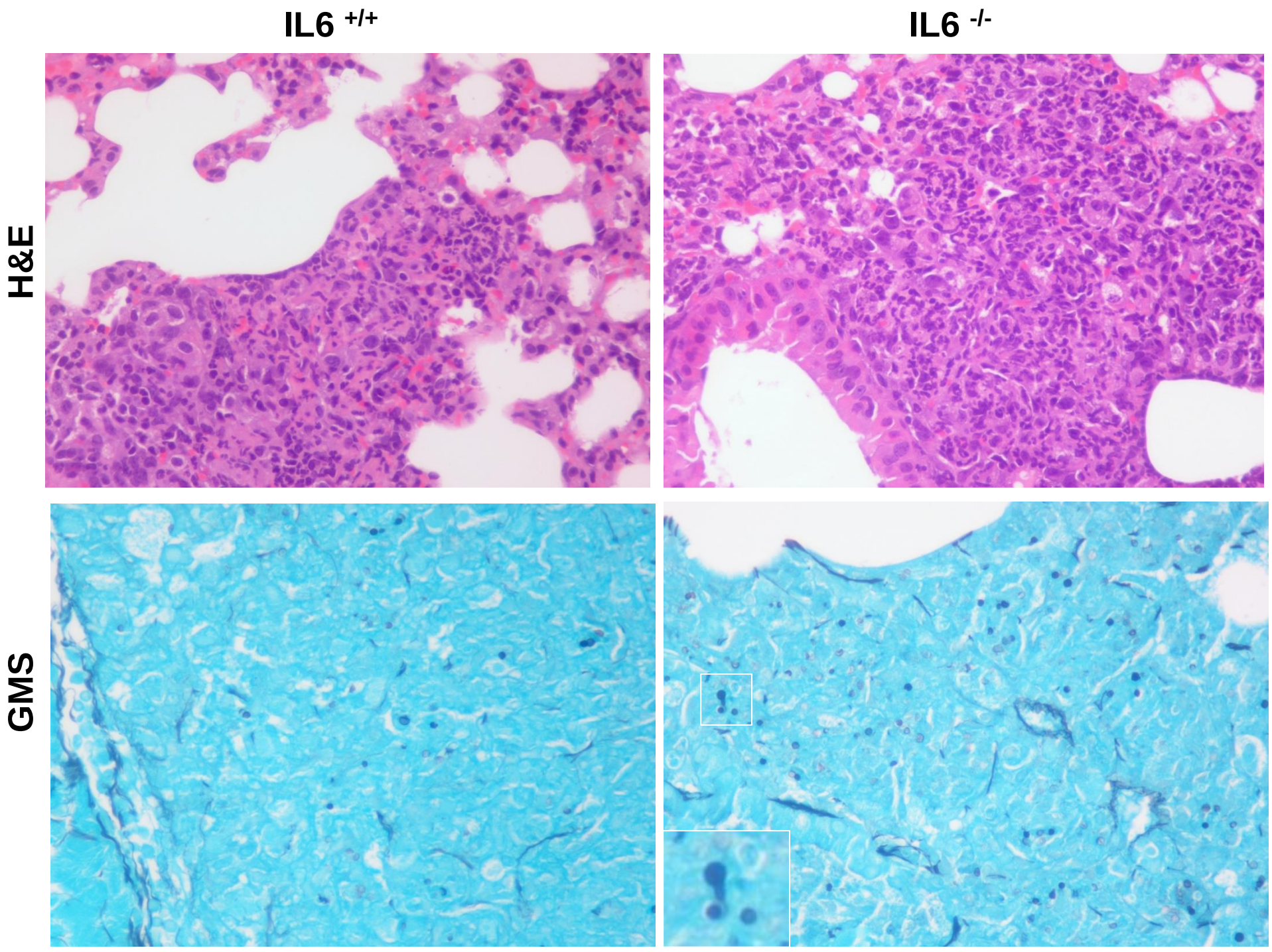

Fig. S4 related to Fig. 3. Histopathological analysis of *Aspergillus* infection in IL6$^{-/-}$ (KO) and control IL-6$^{+/+}$ mice.

IL-6$^{-/-}$ (KO) or control IL-6$^{+/+}$ mice infected *via* intratracheal administration of a standardized inoculum (5 × 10^{7} conidia per mice) of wild type *Aspergillus fumigatus* (ATCC 46645). Mice were sacrificed on Day 3 of infection with *Aspergillus* and representative histopathological sections were stained with H&E or GMS stain to demonstrate fungal elements. In the lungs of IL-6$^{-/-}$ (KO) mice there is evidence of increased numbers of *Aspergillus* dormant and swollen conidia as compared to control IL-6$^{+/+}$ mice. Few germinating conidia are present in the lung of IL-6$^{-/-}$ (KO) mice (shown in inset). Magnification X 400

Fig. S5

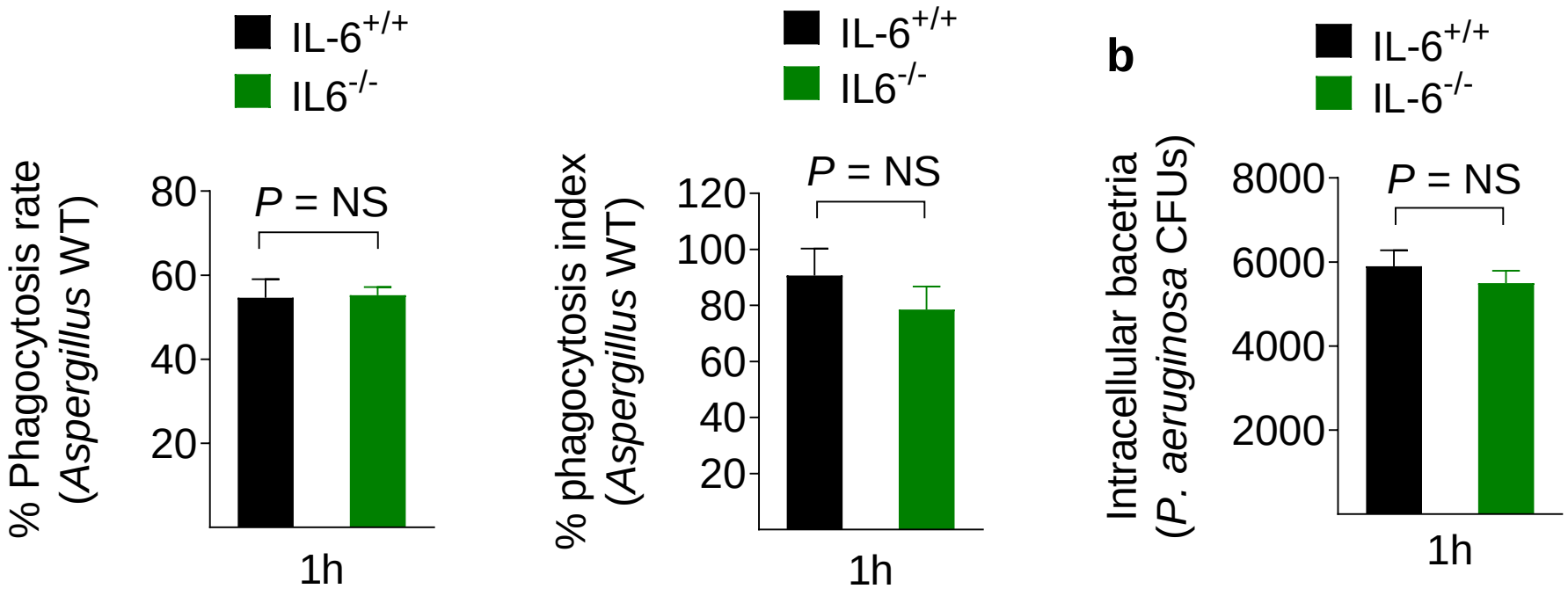
a
IL-6+/+
IL6-/-
% Phagocytosis rate (Aspergillus WT)
80
60
40
20
P = NS
1h
IL-6+/+
IL6-/-
% phagocytosis index (Aspergillus WT)
120
100
80
60
40
20
P = NS
1h
b
IL-6+/+
IL-6-/-
Intracellular bacetria (P. aeruginosa CFUs)
8000
6000
4000
2000
P = NS
1h

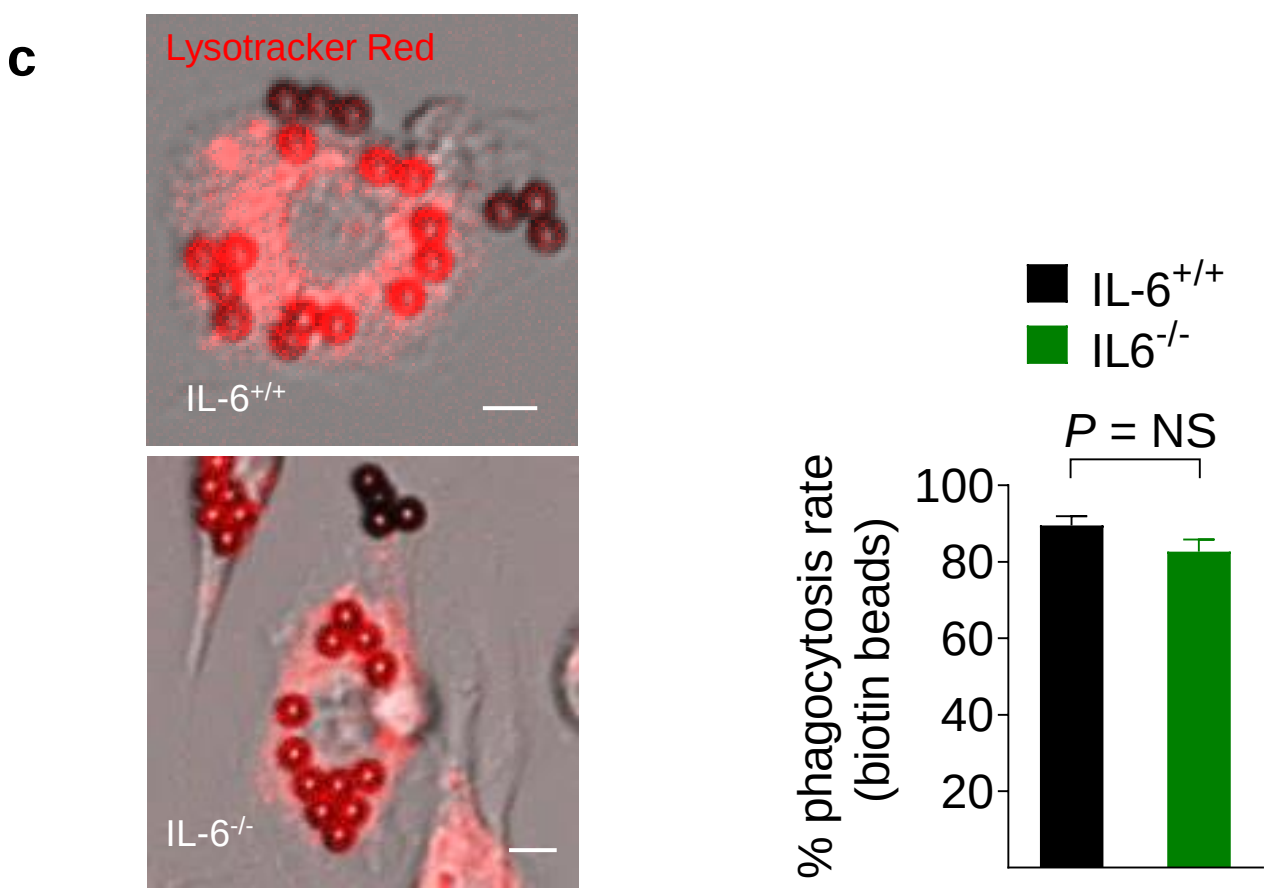
c
Lysotracker Red
IL-6+/+
IL-6-/-
IL-6+/+
IL6-/-
P = NS
% phagocytosis rate (biotin beads)
100
80
60
40
20

Figure S5 related to Fig. 3 and Fig. 4. Analysis of phagocytic capacity in IL6$^{-/-}$ (KO) and control IL-6$^{+/+}$ BMDMs.

(a) BMDMs from IL-6$^{-/-}$ (KO) or control (IL-6$^{+/+}$) mice were infected for 1h with wild type *Aspergillus fumigatus* (ATCC 46645) as in Fig. 3c. Phagocytosis rate and index was assessed by confocal microscopy.

(b) Phagocytosis of *Pseudomonas aeruginosa* (ATCC 27853 strain) following infection of control (IL-6$^{+/+}$) and IL-6 KO (IL-6$^{-/-}$) BMDMs as in Fig. 7h was assessed at 1h. **(c)** BMDMs from IL-6$^{-/-}$ (KO) or control (IL-6$^{+/+}$) mice were stimulated with 3 µm size streptavidin beads coated with biotin (biotin beads) for 1h, stained with Lysotracker Red (to discriminate intracellular particles) and phagocytosis rate was assessed by confocal microscopy. Representative images are shown. Scale bar, 5 µm

Fig. S6

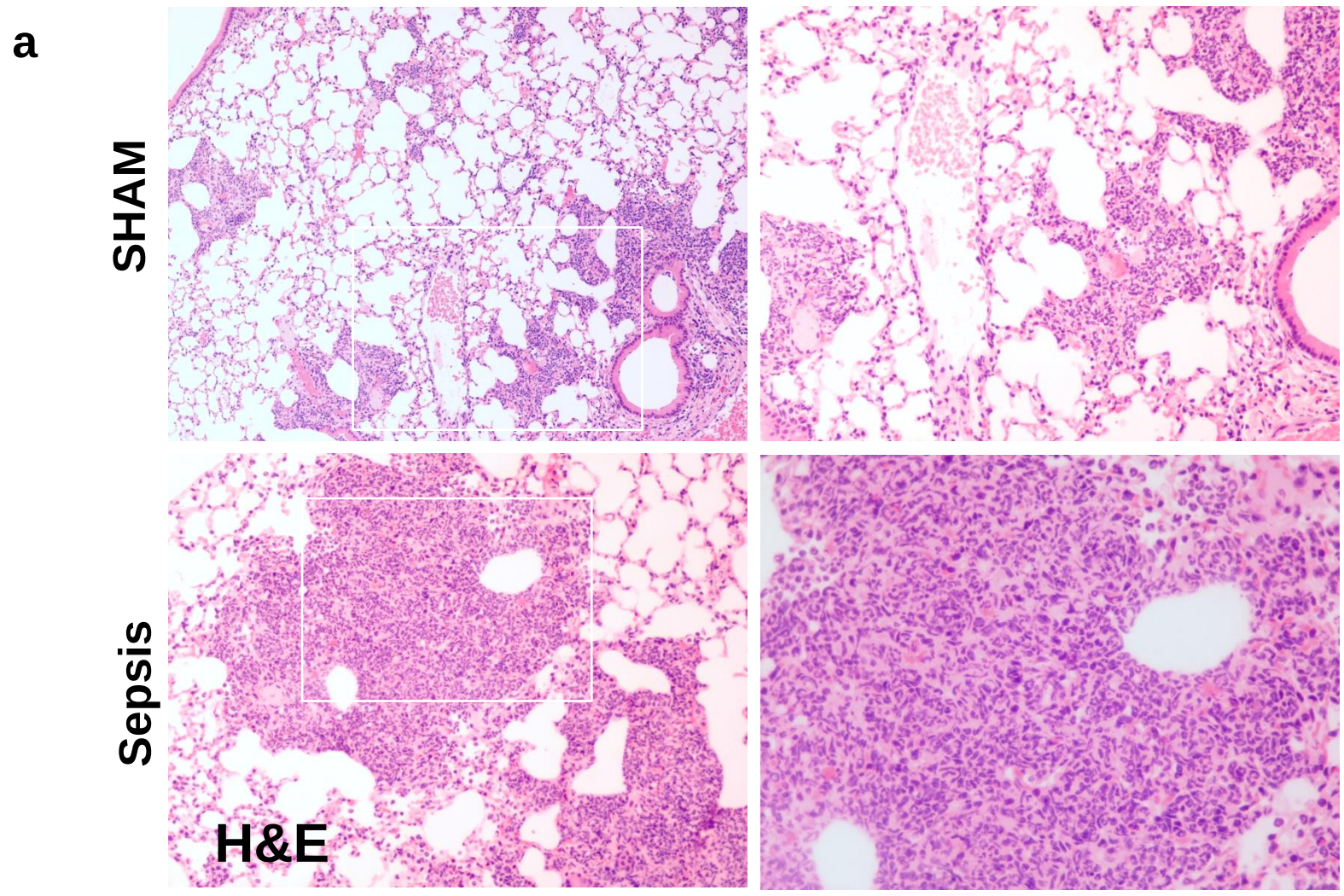
a
SHAM
Sepsis
H&E

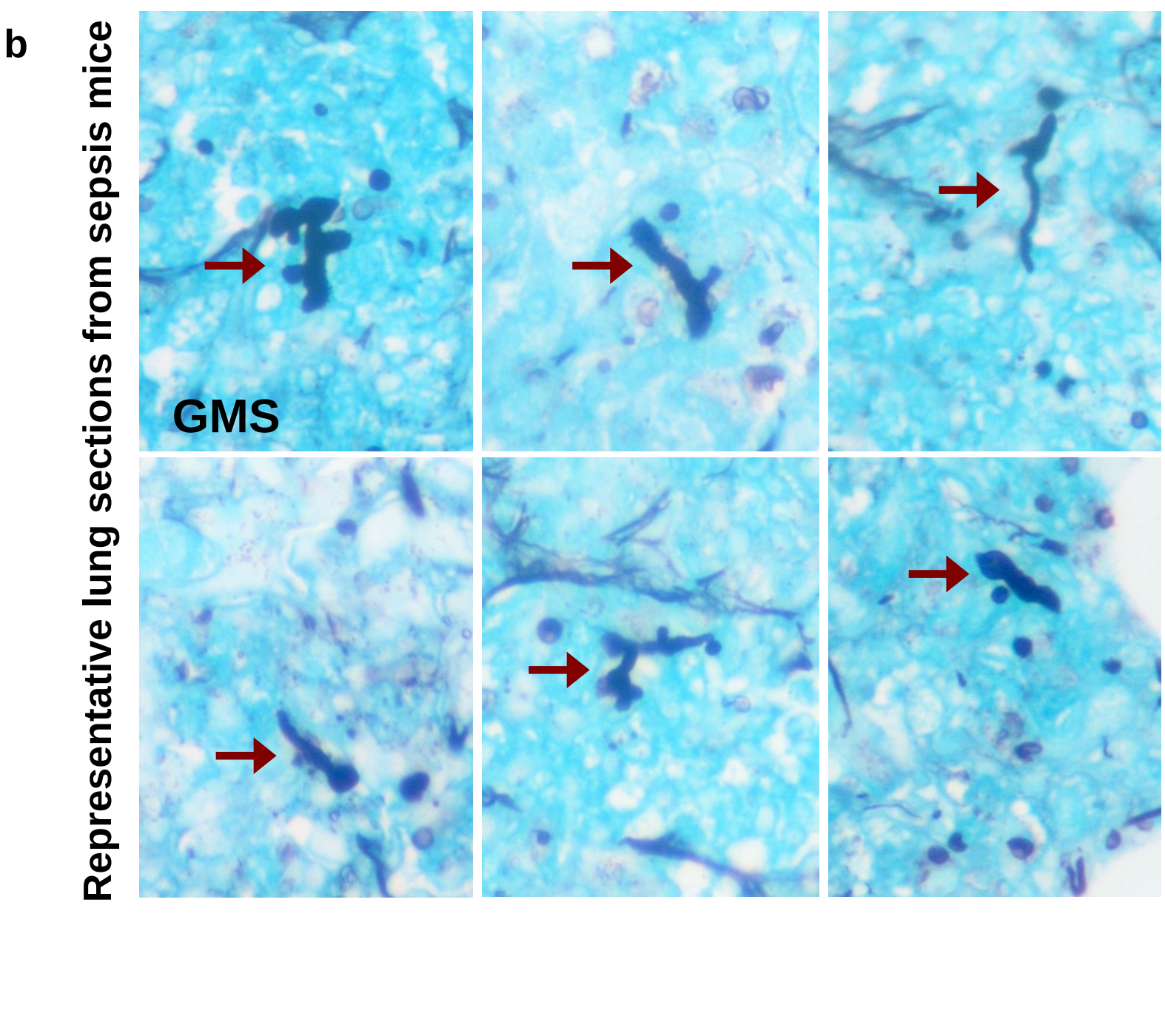
b
Representative lung sections from sepsis mice
GMS

Fig. S6 related to Fig. 5. Histopathological analysis of *Aspergillus* pneumonia in mice recovering from sepsis.

C57BL/6 (B6) mice subjected to severe polymicrobial sepsis (sepsis) or SHAM treated (control) mice were infected via intratracheal administration of a standardized inoculum (5×10^7 conidia per mice) of *Aspergillus fumigatus* wild type clinical isolate (ATCC46645) on Day 7 of recovery from sepsis or SHAM treatment. Mice were sacrificed on Day 3 of infection with *Aspergillus* and representative histopathological sections were stained with **(a)** H&E or **(b)** Grocott-Gomori's Methenamine Silver (GMS) stain to demonstrate fungal elements.

(a) In sepsis mice there is evidence of extensive inflammatory infiltrates by neutrophils and mononuclear phagocytes, consistent with consolidative pneumonia. Localized inflammatory infiltrates are present in SHAM treated mice infected with *Aspergillus*.

(b) Representative lungs sections from sepsis mice with evidence of *Aspergillus* germinating conidia in shown in red arrows. H&E, original magnification X 100. GMS, original magnification X 400

Fig. S7

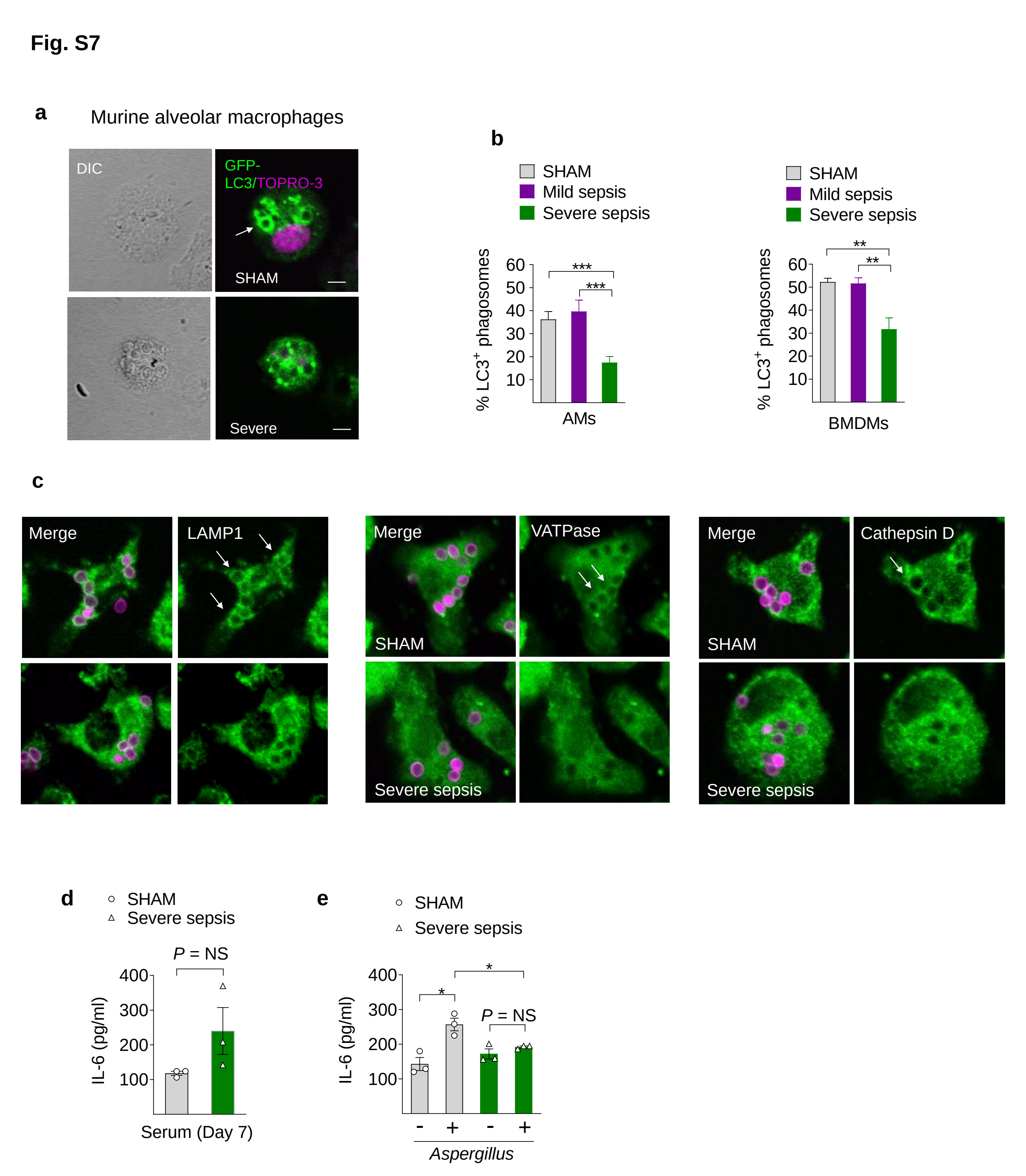
a
Murine alveolar macrophages
DIC
GFP-LC3/TOPRO-3
SHAM
Severe
b
SHAM
Mild sepsis
Severe sepsis
% LC3+ phagosomes
AMs
BMDMs
c
Merge
LAMP1
VATPase
Cathepsin D
SHAM
Severe sepsis
d
SHAM
Severe sepsis
P = NS
IL-6 (pg/ml)
Serum (Day 7)
e
SHAM
Severe sepsis
P = NS
IL-6 (pg/ml)
Aspergillus

Fig. S7 related to Fig. 5 and Fig. 6. Studies on phagosome maturation and IL-6 production in control and sepsis mice.

(a) GFP-LC3 mice were SHAM-treated or subjected to severe or mild bacterial peritonitis and upon recovery (Day 7) infected intratracheally with 5×10^7 conidia of melanin-deficient *Aspergillus ΔpksP* strain. Alveolar macrophages *(*AMs) were isolated from bronchoalveolar lavage at 4h of infected, fixed and analyzed by confocal imaging. Representative fluorescent images of GFP-LC3$^+$ phagosomes from SHAM-treated mice or mice recovering from severe sepsis are shown. LAPosome formation is shown with white arrows. Scale bar 5 μm.

(b) Data on quantification of LC3$^+$ phagosomes in monocytes, BMDMs or alveolar macrophages (AMs) stimulated as in (a) and analyzed by confocal microscopy, are presented as mean ± SEM of three independent experiments. ***p < 0.0001, **p < 0.001, one-way ANOVA and Tukey's multiple comparisons post hoc test.

(c) Representative fluorescent images from BMDMs of control SHAM treated mice or mice recovering from severe sepsis (Day 7) following infection with florescent-labeled *Aspergillus* conidia (shown in magenta), fixation and immunostaining for LAMP1, VATPase, and Cathepsin-D stained with Alexa^{555} secondary antibody (shown in green). Selective localization of each phagosome maturation marker in BMDMs of SHAM treated as compared to BMDMs of severe sepsis mice is evident as a rim of fluorescence surrounding *Aspergillus*-containing phagosomes (white arrows).

(d) IL-6 serum levels in mice following recovery from SHAM treatment or severe sepsis. **(e)** IL-6 production in culture supernatants of BMDMs obtained on Day 7 following recovery from SHAM treatment or severe sepsis, left untreated or following overnight left stimulated with melanin-deficient *Aspergillus ΔpksP* strain at a MOI of 10:1. *p < 0.01, unpaired Student's t test

Table S1 related to Fig. 1. Analysis of secondary infections in patients admitted in the Intensive Care Unit (ICU) with community acquired septic shock

Patient #	% LAPosomes (D7)	LAP status	Secondary Infection	Type of Infection	Type of Pathogen	Day of infection	ICU Center
1	55	Intact LAP	Yes	VAP	*Pseudomonas aeruginosa*	9	University of Crete
4	53	Intact LAP	Yes	VAP	*Klebsiella pneumoniae*	7	University of Crete
5	48	Intact LAP	No			0	University of Crete
6	53	Intact LAP	No			0	University of Crete
7	52	Intact LAP	No			0	University of Crete
8	51	Intact LAP	No			0	University of Crete
14	53	Intact LAP	Yes	VAP	*Serratia marcescens*	10	University of Crete
16	47	Intact LAP	No			0	University of Crete
23	49	Intact LAP	No			0	University of Crete
24	53	Intact LAP	No			0	University of Crete
25	46	Intact LAP	No			0	University of Crete
26	49	Intact LAP	Yes	CVC-related bacteremia	*Acinetobacter baumannii*	12	University of Crete
29	52	Intact LAP	No			0	University of Crete
30	51	Intact LAP	No			0	University of Crete
31	46	Intact LAP	No			0	University of Crete
2	36	Defective LAP	Yes	CVC-related bacteremia	*Acinetobacter baumannii*	8	University of Crete
3	32	Defective LAP	Yes		*Acinetobacter baumannii*	10	University of Crete
9	33	Defective LAP	No			0	University of Crete
11	39	Defective LAP	Yes	VAP	*Stenotrophomonas maltophilia*	6	University of Crete
11	39	Defective LAP	Yes	Bacteremia	*Enterococcus spp.*	8	University of Crete
12	38	Defective LAP	Yes	VAP-bacteremia	*Pseudomonas aeruginosa*	29	University of Crete
12	38	Defective LAP	Yes	Bacteremia	*Klebsiella pneumoniae*	42	University of Crete
13	38	Defective LAP	No			0	University of Crete
18	33	Defective LAP	No			0	University of Crete
22	38	Defective LAP	Yes	CVC-related candidemia	*Candida tropicalis*	19	University of Crete
27	34	Defective LAP	No			0	University of Crete
28	31	Defective LAP	Yes	VAP- bacteremia	*Acinetobacter baumannii*	14	University of Crete
32	42	Defective LAP	No			0	University of Crete
36	39	Defective LAP	No			0	Cochim Hospital, Paris
10	21	Defective LAP	No			0	University of Crete
15	23	Defective LAP	Yes	CVC-related bacteremia	*Pseudomonas aeruginosa*	3	University of Crete
17	14	Defective LAP	Yes	CVC-related bacteremia	*Staphylococcus epidermidis*	10	University of Crete
19	16	Defective LAP	Yes	New sepsis episode (UTI)	*Escherichia coli*	21	University of Crete
20	20	Defective LAP	Yes	Sepsis, CVC-related bacteremia	*Escherichia coli*	16	University of Crete
20	20	Defective LAP	Yes	CVC-related bacteremia	CoNS	25	University of Crete
21	8	Defective LAP	Yes	CVC-related bacteremia	*Acinetobacter baumannii*	18	University of Crete
21	8	Defective LAP	Yes	CVC-related candidemia	*Candida tropicalis*	35	University of Crete
21	8	Defective LAP	Yes	Bacteremia	*Klebsiella pneumoniae*	85	University of Crete
33	18	Defective LAP	Yes	VAP	*Klebsiella pneumoniae*	18	University of Crete
34	24	Defective LAP	No	N/A		0	University of Crete
35	18	Defective LAP	Yes	CVC-related candidemia	*Candida* spp.	16	University of Crete
37	28	Defective LAP	No	N/A		0	Cochim Hospital, Paris
38	16	Defective LAP	No	N/A		0	Cochim Hospital, Paris
39	42	Defective LAP	Yes	VAP	*Acinetobacter baumannii*	13	University of Crete
39	42	Defective LAP	Yes	CVC-related candidemia	*Candida parapsilosis*	44	University of Crete
39	42	Defective LAP	Yes	CVC-related bacteremia	*Acinetobacter baumannii*	45	University of Crete
39	42	Defective LAP	Yes	VAP	*Pseudomonas aeruginosa*	53	University of Crete
40	31	Defective LAP	Yes	Bacteremia	*Pseudomonas aeruginosa*	7	University of Crete
41	26	Defective LAP	Yes	VAP-bacteremia	*Acinetobacter baumannii*	38	University of Crete
42	22	Defective LAP	Yes	VAP	*Acinetobacter baumannii*	7	University of Crete
42	22	Defective LAP	Yes	Bacteremia	*Klebsiella pneumoniae*	11	University of Crete
42	22	Defective LAP	Yes	New sepsis episode	*olymicrobial intraabdominal sepsis*	13	University of Crete
43	36	Defective LAP	No			0	University of Crete

Table S2 related to Fig. 1. Analysis of cytokine responses in monocytes of sepsis patients with different degree of LAP responses following stimulation with *Aspergillus*

Pt #	% LC3+ phagosomes (	IL-1b (D1)	IL-1b (D7)	IL-1Ra (D1)	IL-1Ra (D7)	TNF (D1)	TNF (D7)	IL-6 (D1)	IL-6 (D7)
1	55	N/A	N/A	N/A	N/A	N/A	N/A	N/A	N/A
4	53	628	608	12867	33996	150	196	8805	9017
5	48	63	167	11127	27565	122	306	313	696
6	53	230	202	50943	34027	433	625	175	409
7	52	2107	610	58893	71051	410	433	8805	2554
8	51	134	421	14772	27110	116	387	751	1406
14	53	39	481	10400	9764	78	792	627	3817
16	47	N/A	1705	N/A	40311	N/A	819	N/A	4000
23	49	1022	665	18037	9755	1150	821	10708	2265
24	53	246	218	10060	10653	328	429	1331	1275
25	46	154	553	8888	22520	532	257	1379	5716
26	49	293	42	8968	3637	1053	228	2333	208
29	52	18	87	6989	780	86	171	251	9
30	51	129	170	12865	16643	202	133	166	456
31	46	308	329	19896	20314	305	444	890	486
2	36	386	277	30890	36056	148	121	6873	3252
3	32	160	39	28352	8061	129	89	710	31
9	33	144	175	40561	25577	550	124	372	365
11	39	133	76	19060	14355	407	245	855	99
12	38	39	168	12857	39417	78	194	221	1245
13	38	N/A	592	N/A	21152	N/A	565	N/A	4000
18	33	N/A	N/A	N/A	N/A	N/A	N/A	N/A	N/A
22	38	761	285	25869	27836	1023	397	12000	2713
27	34	170	750	6805	10060	381	902	2295	2794
28	31	N/A	N/A	N/A	N/A	N/A	N/A	N/A	N/A
32	42	704	107	6897	7529	672	133	1105	228
36	39	81	37	N/A	N/A	153	87	119	37
10	21	50	122	26976	92412	223	851	301	765
15	23	N/A	39	N/A	14433	N/A	78	N/A	195
17	14	N/A	N/A	N/A	N/A	N/A	N/A	N/A	N/A
19	16	N/A	N/A	N/A	N/A	N/A	N/A	N/A	N/A
20	20	N/A	195	N/A	22456	N/A	136	N/A	633
21	8	N/A	N/A	N/A	N/A	N/A	N/A	N/A	N/A
33	18	N/A	N/A	N/A	N/A	N/A	N/A	N/A	N/A
34	24	N/A	N/A	N/A	N/A	N/A	N/A	N/A	N/A
35	18	N/A	N/A	N/A	N/A	N/A	N/A	N/A	N/A
37	28	15	16	N/A	N/A	68	43	20	16
38	16	77	93	N/A	N/A	183	191	187	93

Table S3 related to Fig. 1. Analysis of demographic, clinical and microbiological characteristics of patients with septic shock

Pt #	% LAPosomes (D7)	SEX	AGE	SEPSIS SOURCE	Identified Pathogen	APACHE II score	SOFA D1	Sofa D7	days in ICU	Mortality in ICU
1	55	F	71	Pneumonia	*Proteus spp.*	24	14	9	42	YES
4	53	F	65	Intra-abdominal		19	6	3	48	YES
5	48	M	84	Intra-abdominal		23	10	6	23	NO
6	53	M	70	Intra-abdominal		21	5	4	9	NO
7	52	F	49	Intra-abdominal		8	3	2	5	NO
8	51	F	47	Intra-abdominal		21	9	5	21	NO
14	53	M	85	Intra-abdominal		18	8	15	16	YES
16	47	F	43	Urinary tract infection		26	15	3	9	NO
23	49	M	68	Intra-abdominal		21	16	15	12	YES
24	53	F	58	Intra-abdominal		23	11	1	7	NO
25	46	M	84	Intra-abdominal		19	9	8	14	YES
26	49	M	74	Intra-abdominal		14	8	13	13	YES
29	52	M	79	Intra-abdominal		23	8	10	21	NO
30	51	M	79	Pneumonia	*Klebsiella pneumoniae*	21	10	4	9	NO
31	46	M	26	Urinary tract infection	*Providencia spp.*	20	13	5	8	NO
2	36	M	46	Intraabdominal		18	7	7	21	NO
3	32	M	68	Intraabdominal		40	7	7	14	YES
9	33	M	45	Intraabdominal		16	8	2	9	NO
11	39	M	71	Pneumonia		31	10	9	21	NO
12	38	F	58	Pneumonia		18	8	11	48	YES
13	38	F	50	Intra-abdominal		13	7	7	11	NO
18	33	M	78	Pneumonia-empyema	*Serratia marcescens*	12	5	4	44	NO
22	38	M	74	Pneumonia-bacteremia	*Klebsiella pneumoniae*	23	10	12	17	YES
27	34	M	37	Intra-abdominal		21	12	10	17	NO
28	31	M	66	Pneumonia-bacteremia	*Streptococcus pneumoniae*	35	12	13	22	NO
32	42	M	63	Intra-abdominal		16	9	4	4	NO
36	39	M	71	Intra-abdominal-bacteremia	*Pseudomonas aeruginosa, Enterococccus faecalis*	37	15	N/A	26	NO
10	21	M	66	Pneumonia	*Escherichia coli*	31	13	6	14	NO
15	23	F	42	Streptococcal Toxic Shock Syndrome	*Streptococcus pyogenes*	22	12	9	12	NO
17	14	M	72	Intra-abdominal		31	6	1	5	NO
19	16	M	69	Urinary tract infection-meningitis	*Escherichia coli*	30	14	7	20	NO
20	20	F	87	Intra-abdominal		21	11	9	16	YES
21	8	M	54	Intra-abdominal		27	9	11	104	YES
33	18	F	49	Intra-abdominal	*Escherichia coli*	13	12	8	23	NO
34	24	M	57	Intra-abdominal		17	9	4	10	NO
35	18	M	56	Skin and Soft Tissue Infection (Fasciitis)		17	10	5	11	NO
37	28	F	65	Pneumonia		39	14	N/A	12	NO
38	16	F	59	Pneumonia		29	7	N/A	16	NO
39	42	M	79	Pneumonia		23	7	8	85	YES
40	31	M	79	Pneumonia		24	10	10	10	YES
41	26	M	76	Pneumonia	*Pseudomonas aeruginosa*	40	17	21	7	YES
42	22	M	57	Intra-abdominal		14	3	8	53	YES
43	36	F	42	Urinary tract infection	*Proteus spp.*	19	15	15	17	NO

Data S1

a

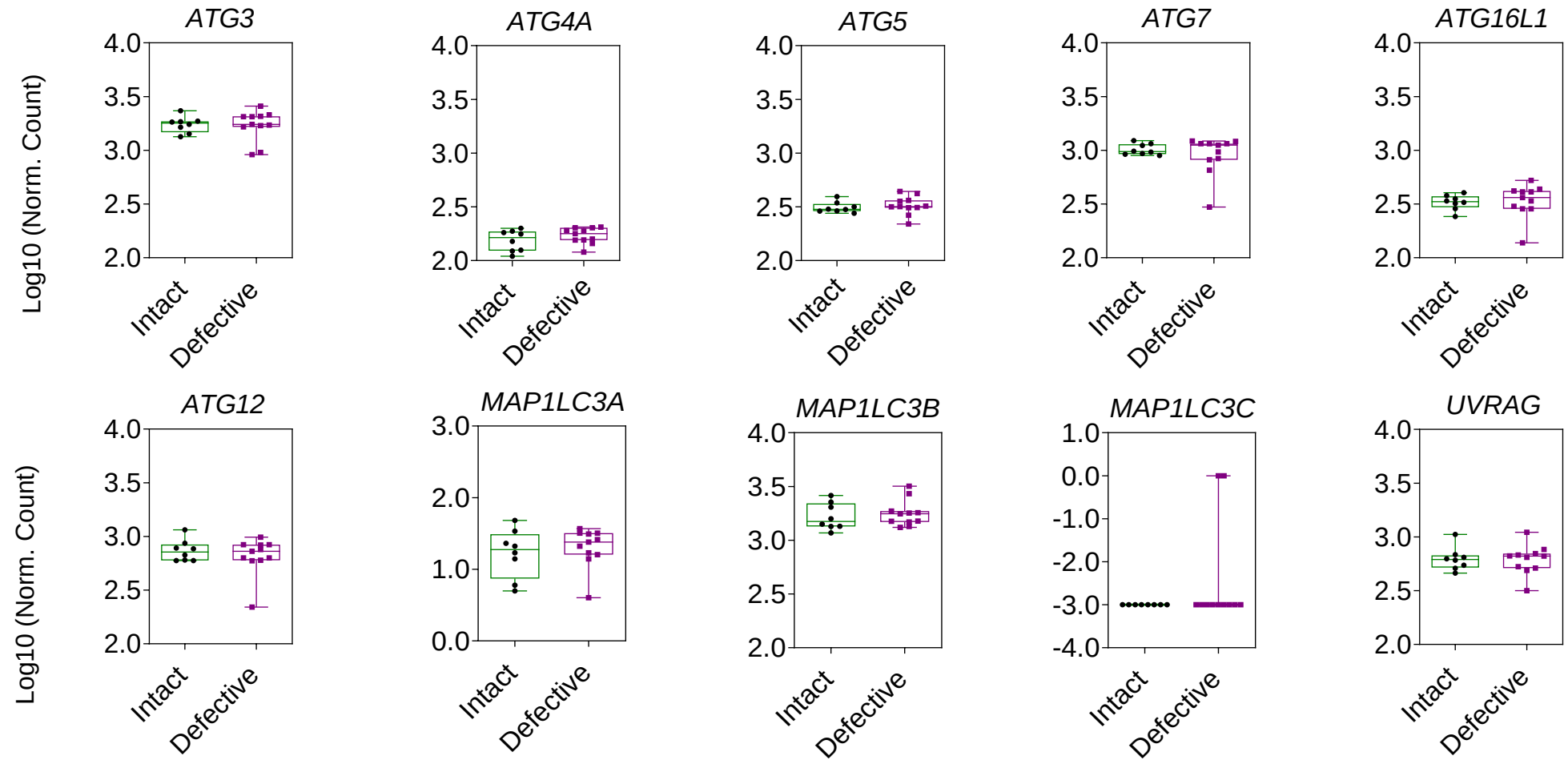
ATG3
ATG4A
ATG5
ATG7
ATG16L1
ATG12
MAP1LC3A
MAP1LC3B
MAP1LC3C
UVRAG
Log10 (Norm. Count)
Intact
Defective

b

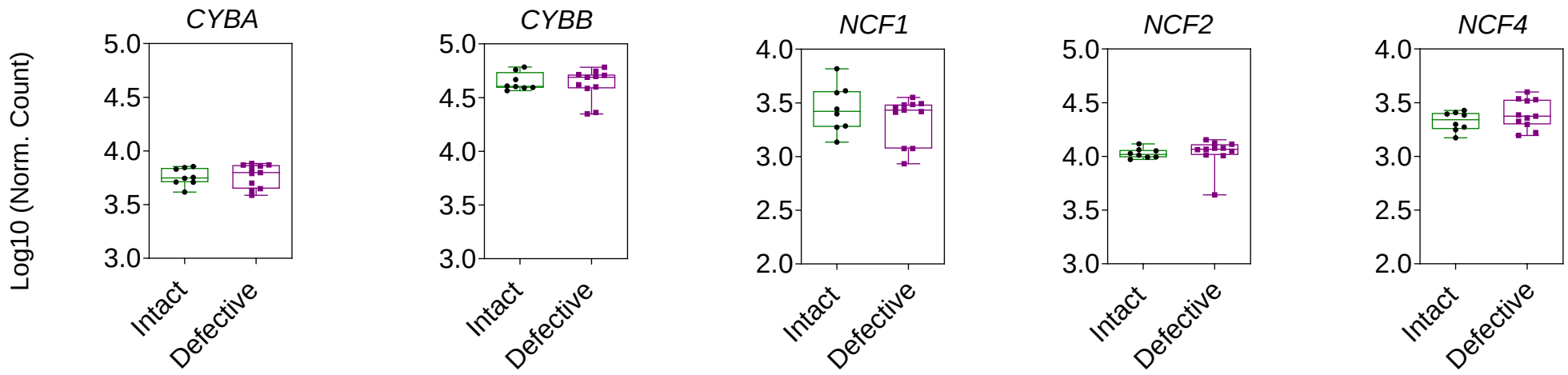
CYBA
CYBB
NCF1
NCF2
NCF4
Log10 (Norm. Count)
Intact
Defective

c

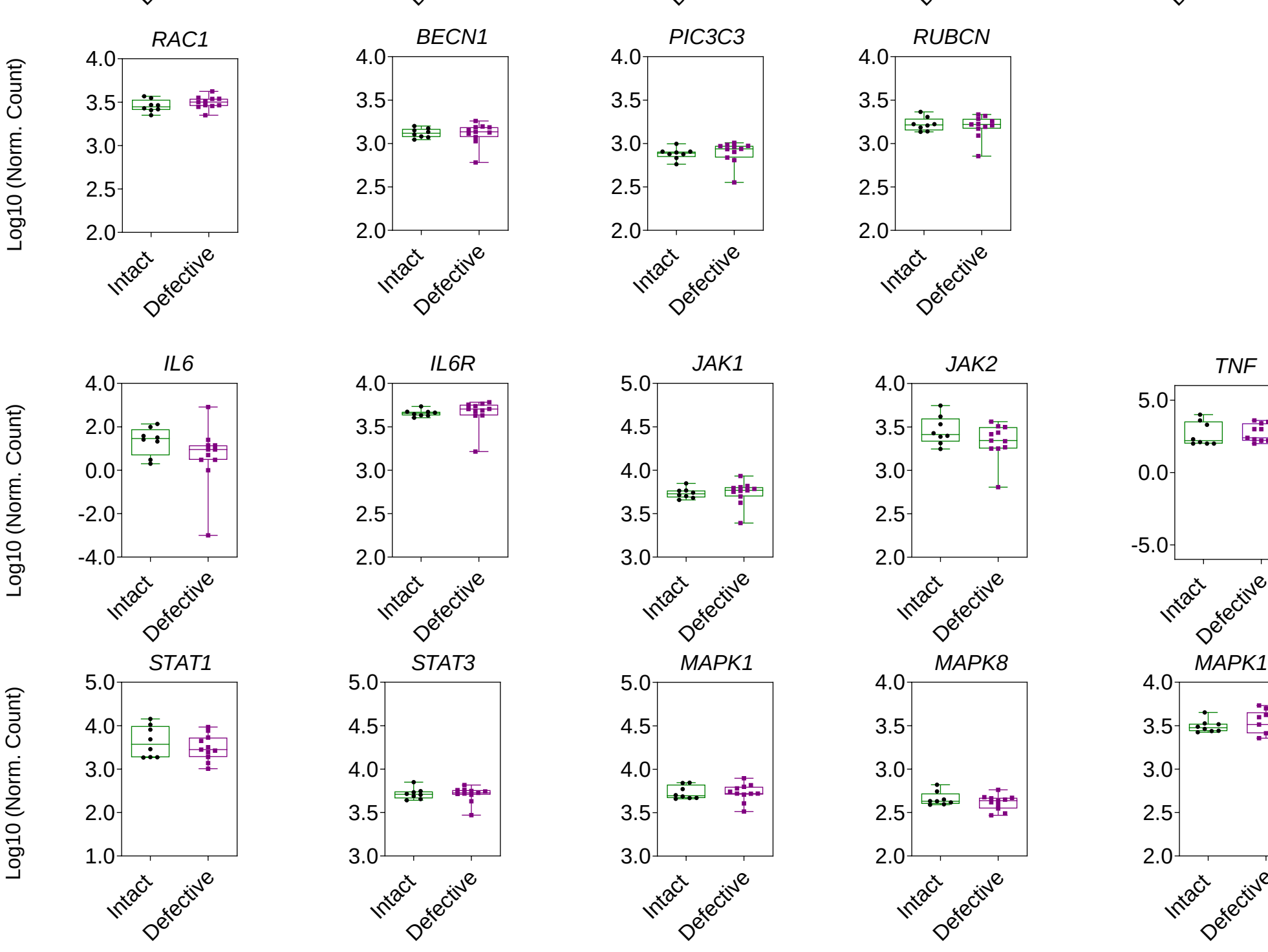
RAC1
BECN1
PIC3C3
RUBCN
IL6
IL6R
JAK1
JAK2
TNF
STAT1
STAT3
MAPK1
MAPK8
MAPK14
Log10 (Norm. Count)
Intact
Defective

Data S1 related to Fig. 1. RNAseq analysis of selected genes in human sepsis monocytes.

Transcriptomics analysis of genes regulating **(a)** general autophagy, **(a, b)** LAP, and **(c)** Cytokine signaling in unstimulated monocytes of sepsis patients with or without defective LAP responses following sepsis recovery (Day 7). Data on expression of individual genes are expressed with whisker boxes. Distributions of the RNAseq datasets using Box plot representations. "Box plots representing expression level distributions (log10 of normalized counts) for all genes in the different groups of patients.

Data S2

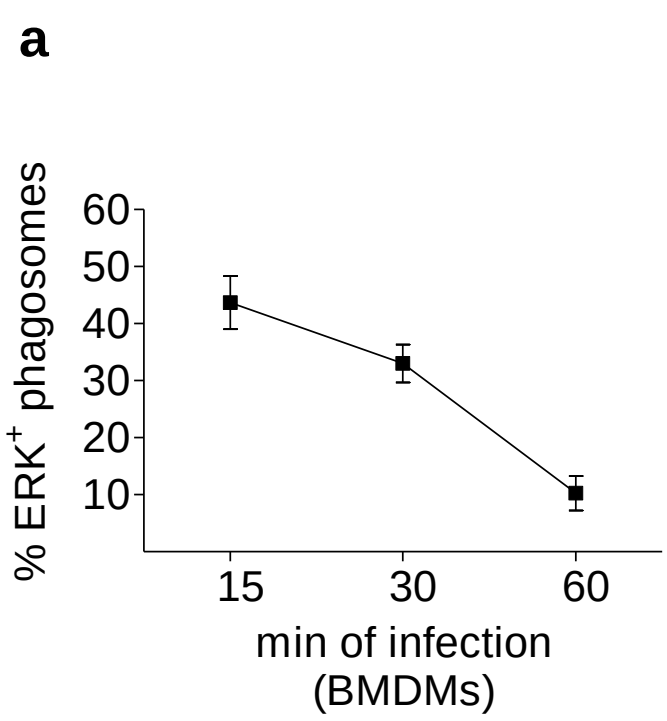
a
% ERK+ phagosomes
60
50
40
30
20
10
15
30
60
min of infection
(BMDMs)

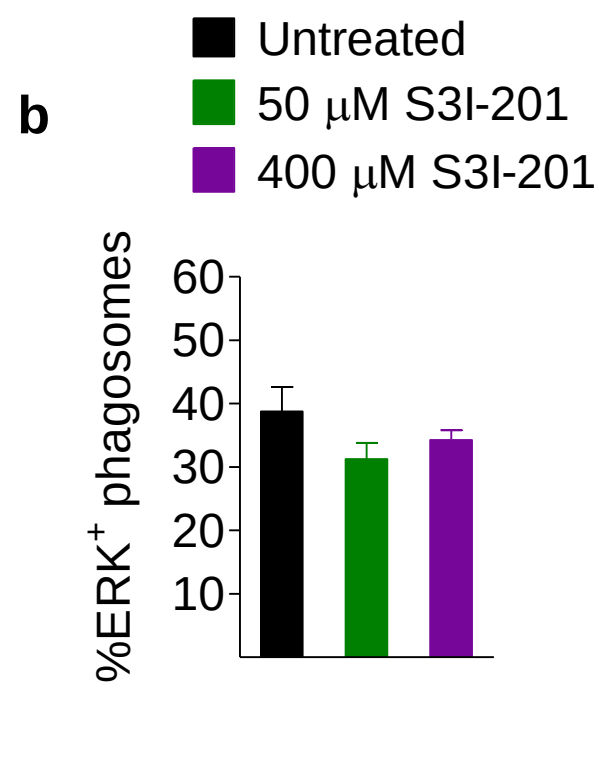
b
Untreated
50 μM S3I-201
400 μM S3I-201
%ERK+ phagosomes
60
50
40
30
20
10

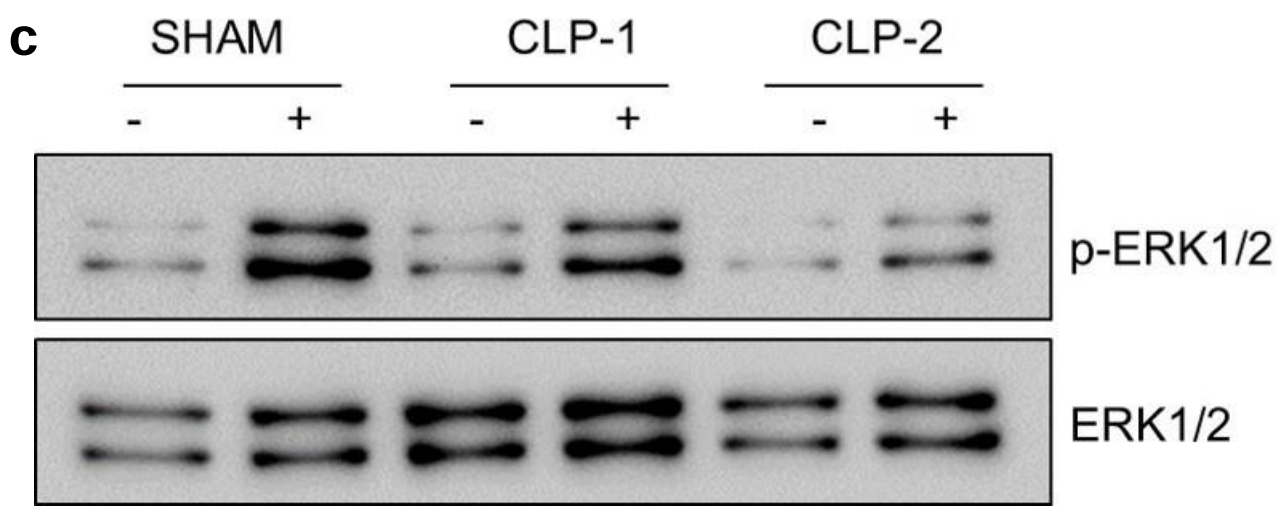
c
SHAM
CLP-1
CLP-2
-
+
-
+
-
+
p-ERK1/2
ERK1/2

Data S2 related to Fig. 4 and Fig. 6. Studies on activation of ERK1/2 signaling in BMDMs of mice recovering from sepsis.

(a) Data on kinetics of ERK recruitment in the phagosome of BMDMs obtained from C57BL/6 (B6) mice at different time point of infection with *Aspergillus* conidia (MOI 3:1), presented as as mean ± SEM of three independent experiments.

(b) BMDMs from C57BL/6 (B6) mice left untreated, or treated with STAT3 inhibitor (S3I-201) and infected as in Fig. 4f. Data on quantification of ERK^{+} phagosomes are presented as mean ± SEM of one out of three independent experiments.

(c) BMDMs from SHAM treated mice or mice recovering from severe sepsis (CLP1, 2) were left untreated or infected for 20 min with *Aspergillus* and phosphorylation of ERK1/2 was determined in cell lysates by immunoblot analysis. ERK1/2 was used as loading control.

Movie S1 related to Fig. 4. Time-lapse video of *Aspergillus* phagosome transport in BMDMs of IL-6$^{+/+}$ (control) mice. Overlaid in cyan is the trajectory of a representative phagosome from the beginning of the time series to the last shown frame.

Movie S2 related to Fig. 4. Time-lapse video of *Aspergillus* phagosome transport in BMDMs of IL-6$^{-/-}$ (KO) mice. Overlaid in green is the trajectory of a representative phagosome from the beginning of the time series to the last shown frame.